Electronic Supplementary Material (ESI) for Journal of Materials Chemistry C.

Supporting information for:

Inverted organic photovoltaics with a solution processed ZnO/MgO electron transport bilayer

Ioannis Ierides[a], Isaac Squires[a], Giulia Lucarelli[b], Thomas M. Brown[b] and Franco Cacialli[a]

[a]Department of Physics and Astronomy and London Centre for Nanotechnology, University College London, London, WC1H 0AH, United Kingdom

[b]CHOSE (Centre for Hybrid and Organic Solar Energy), University of Rome Tor Vergata, Italy.

S1. Supplementary information for experimental techniques

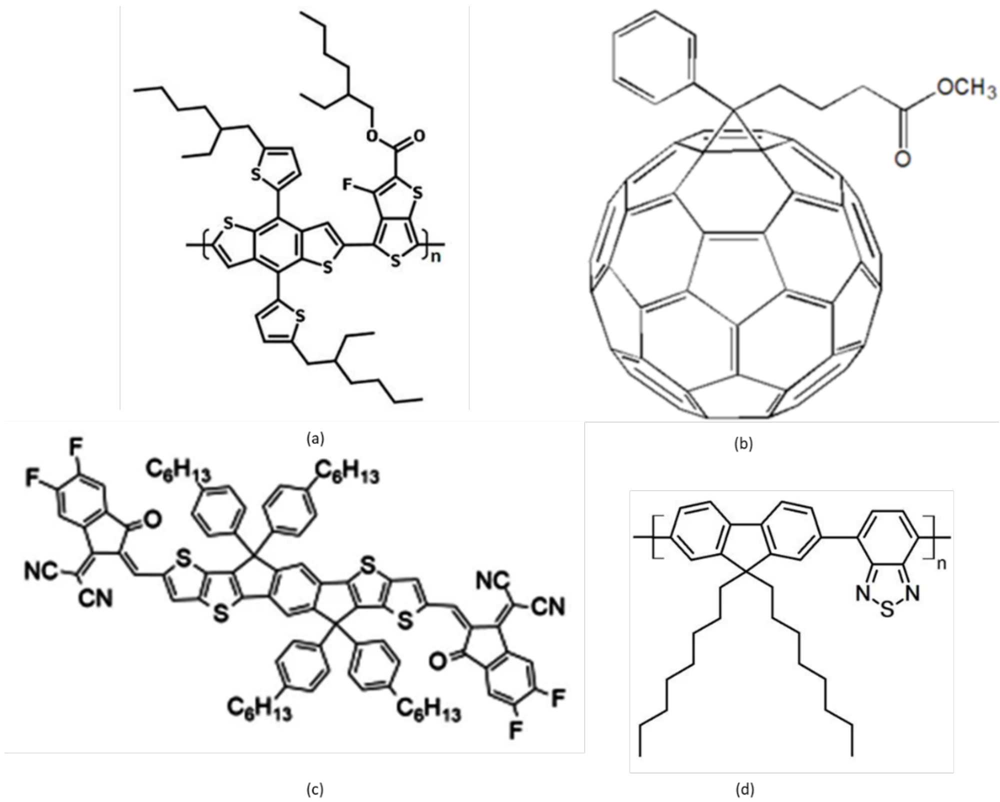

Figure S1: The chemical structures of (a) PTB7-Th, (b) $PC_{70}BM$, (c) ITIC-2F and (d) F8BT.

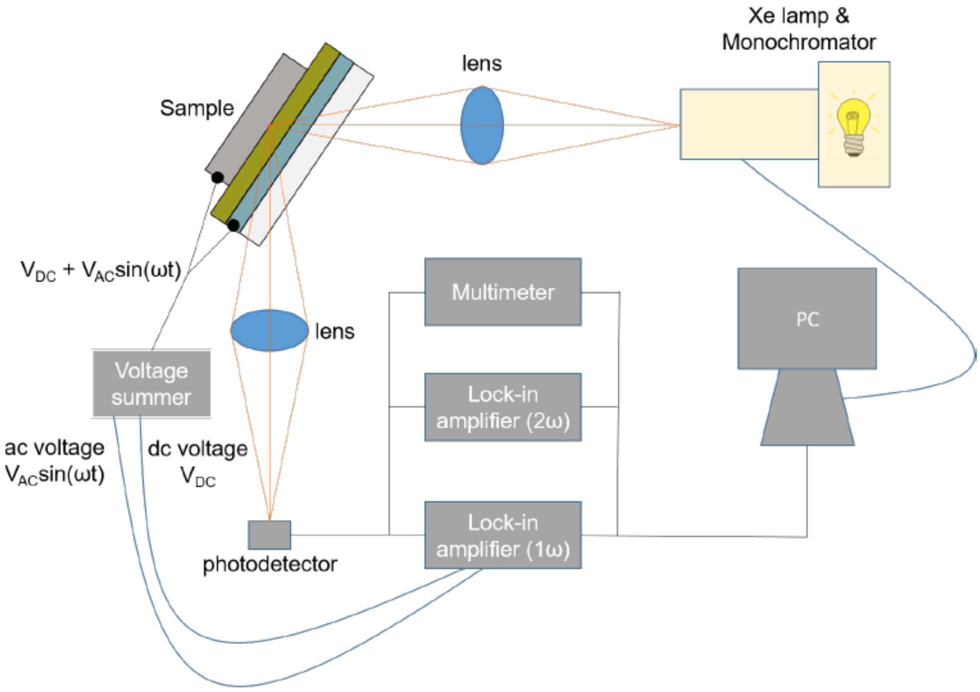

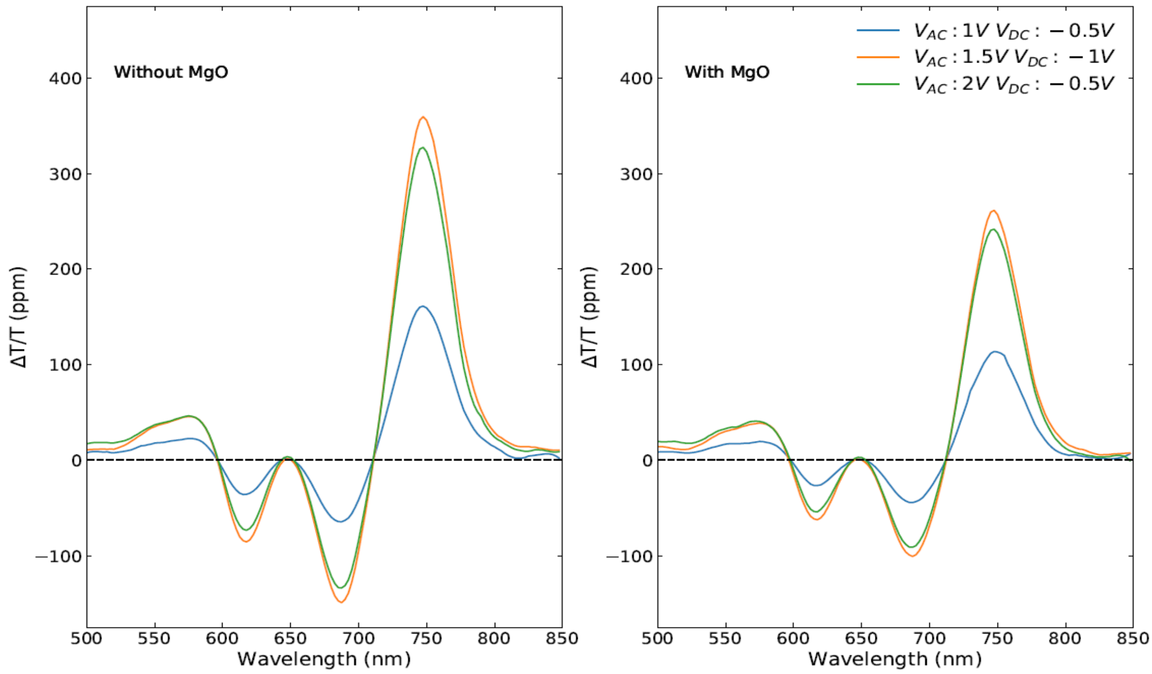

Figure S2: The schematic of the home-built electroabsorption set up used in the investigations (top panel) and representative examples of testing the validity of extracting the built-in voltage from the ITO/ZnO/[with/without MgO(10 nm)]/PTB7-Th:PC_{70}BM/Au devices used in the study . Note the isosbestic point occurrence at points where the electroabsorption signal is null.

S2. Supplementary materials to Results and Discussion

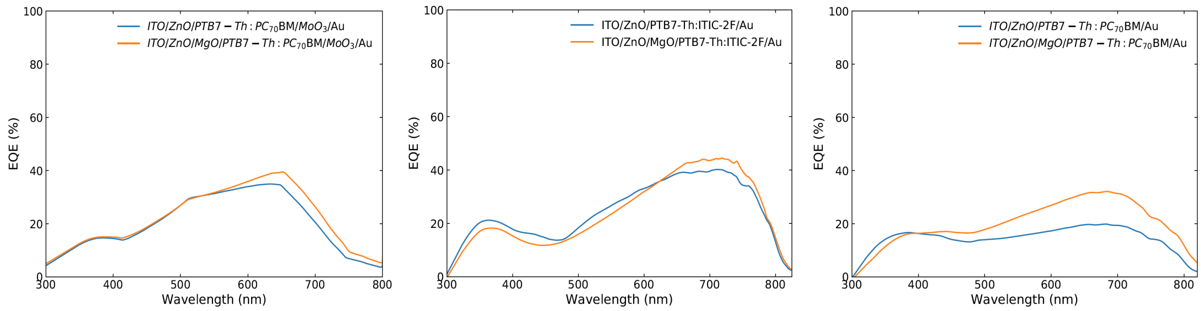

Figure S3: Representative EQE curves of the bilayer ZnO/MgO ETL vs the single ZnO ETL. The thickness of the MgO layer in the relevant devices is ~ 10 nm.

Sample	**Calculated J_{sc} (mAcm^{-2})**
ITO/ZnO/PTB7-Th:$PC_{70}BM$/MoO_3/Au	10.5 ± 0.7
ITO/ZnO/**MgO (10 nm)** /PTB7-Th:$PC_{70}BM$/ MoO_3/Au	11.0 ± 0.7
ITO/ZnO/PTB7-Th:$PC_{70}BM$/Au	8.5 ± 0.7
ITO/ZnO/**MgO (10 nm)**/PTB7-Th:$PC_{70}BM$/Au	8.7± 0.7
ITO/ZnO/PTB7-Th:ITIC-2F/Au	9.7 ± 0.7
ITO/ZnO/**MgO (10 nm)**/PTB7-Th:ITIC-2F/Au	10.7 ± 0.7

Table S1: The extracted J_{sc} from the EQE curves using the AM1.5 spectrum. The MgO precursor was deposited by spin-coating at 5000 rpm in all cases (corresponding to a final thickness ~ 10 nm).

The higher EQE values for the ZnO/MgO device compared to the ZnO-only device are in agreement with the expectations from the J_{sc} under illumination. The theoretical J_{sc} has been calculated from the spectra and matches the experimental J_{sc} as expected.

Sample	**PCE (%)**	**J_{sc} (mAcm^{-2})**	**V_{oc} (V)**	**FF**
ITO/ZnO/PTB7-Th:$PC_{70}BM$/MoO_3/Ag	3.44 ± 0.18	10.1 ± 0.4	0.72 ± 0.01	0.45 ± 0.02
ITO/ZnO/**MgO (10 nm)**/PTB7-Th:$PC_{70}BM$/ MoO_3/Ag	3.61 ± 0.34	10.6 ± 0.4	0.72 ± 0.01	0.47 ± 0.02
ITO/ZnO/PTB7-Th:$PC_{70}BM$/Au	1.61 ± 0.09	8.9 ± 0.4	0.46 ± 0.01	0.39± 0.01
ITO/ZnO/**MgO (10 nm)**/PTB7-Th:$PC_{70}BM$/Au	1.75 ± 0.06	9.2 ± 0.2	0.46 ± 0.01	0.41± 0.01
ITO/ZnO/PTB7-Th:ITIC-2F/Au	2.03 ± 0.24	10.5 ± 0.7	0.44 ± 0.01	0.44 ± 0.02
ITO/ZnO/**MgO (10 nm)**/PTB7-Th:ITIC-2F/Au	2.31 ± 0.17	10.7 ± 0.7	0.44 ± 0.01	0.49± 0.01
ITO/SnO_2/PTB7-Th:$PC_{70}BM$/Au	1.44	9.34	0.64	0.24
ITO/SnO_2/**MgO (10 nm)** /PTB7-Th:$PC_{70}BM$/Au	2.08	10.54	0.61	0.32

Table S2: Variation in key photovoltaic parameters of OPVs based on a single ETL vs the bilayer ETL.

Devices that do not incorporate MoO_3 show lower performance, clearly demonstrating the notion that in addition to a good ETL, the inclusion of a HTL is also crucial to achieve high efficiency in OPVs. Note that the non-fullerene acceptor device efficiencies are limited since a HTL is absent for these devices.

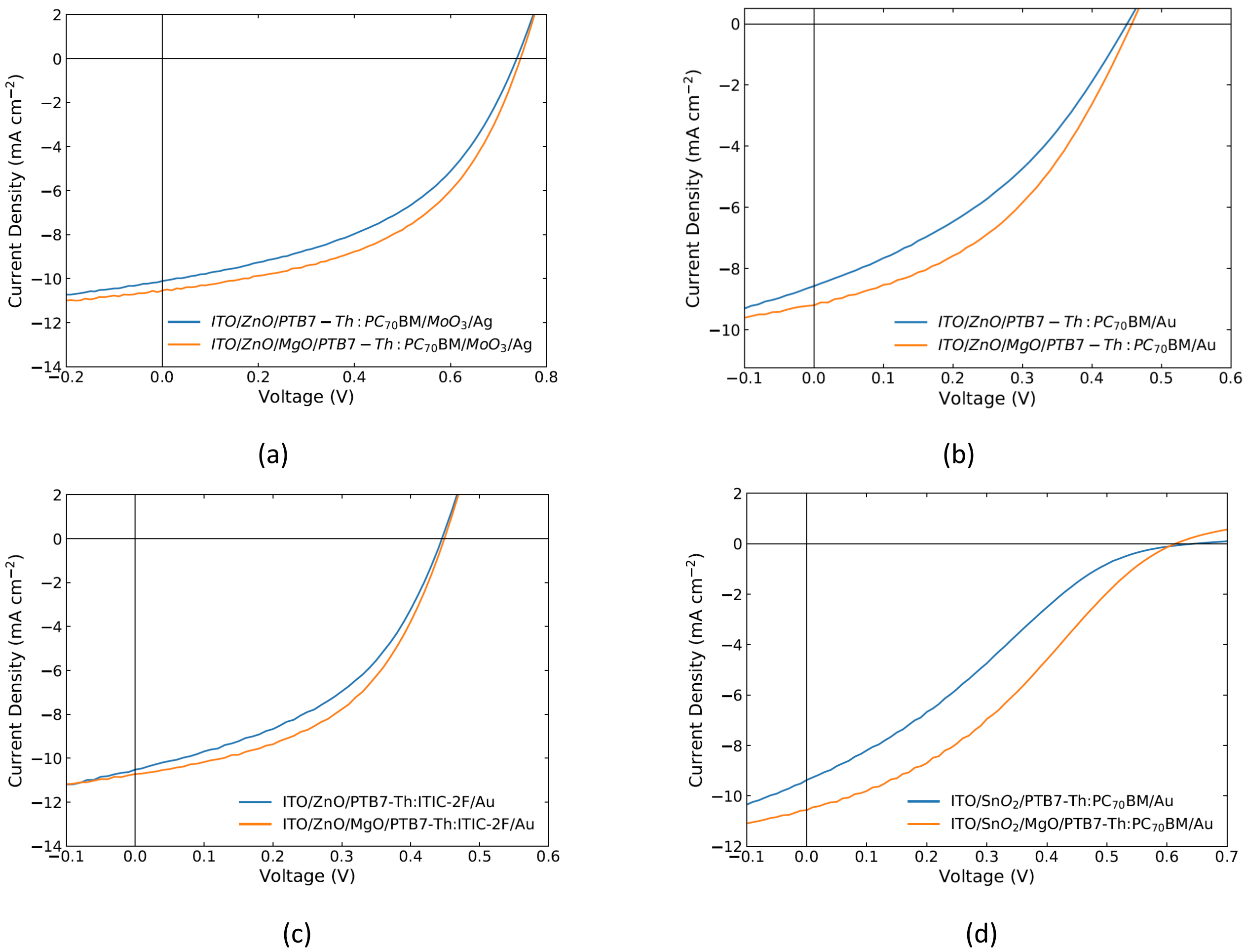

Figure S4: Representative current-voltage curves demonstrating the success of the bilayer MgO ETL vs a single ETL for various OPV architectures. Measurements are taken under 1 sun. (a) Au top contact substituted with Ag. (b) Devices without the MoO_3 HTL. (c) Devices with a blend containing the non-fullerene acceptor ITIC-2F rather than $PC_{70}BM$ as the acceptor. (d) SnO_2 ETL based devices, intentionally not optimised, to emphasise that beneficial effects of MgO can be obtained even without strict preparation protocols. The thickness of the MgO layer is ~10 nm (precursor deposited at 5000 rpm).

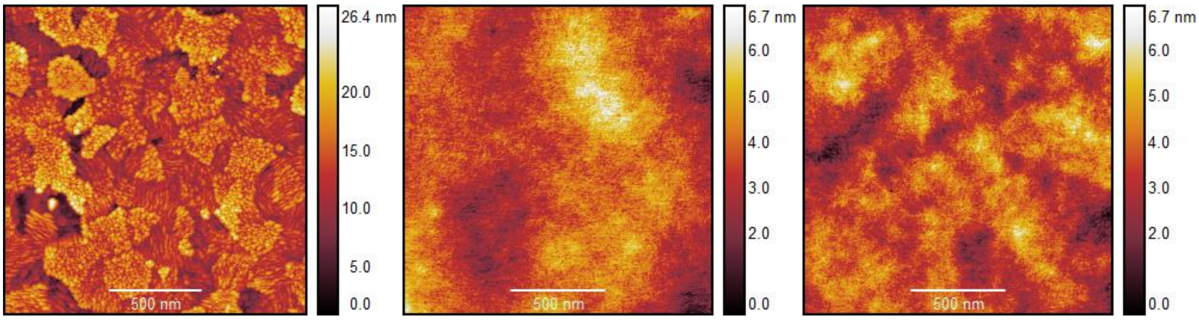

Figure S5: Tapping mode AFM images of the topography of ITO, ITO/PTB7-Th:$PC_{70}BM$, ITO/MgO(10 nm)/PTB7-Th:$PC_{70}BM$.

Sample	**Mean Square Roughness (nm)**
ITO/PTB7-Th:$PC_{70}BM$	0.7 ± 0.1
ITO/**MgO(10 nm)**/PTB7-Th:$PC_{70}BM$	0.7± 0.1

Table S3: Mean Square Roughness of the topography of samples imaged via AFM. (MgO layer thickness ~ 10 nm).

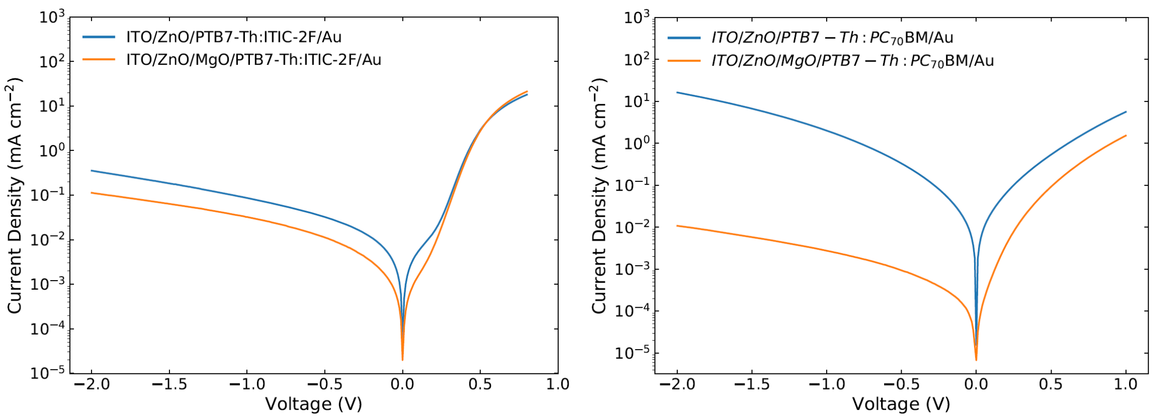

Figure S6: Representative current-voltage curves recorded in the dark showing the variation in leakage current between the bilayer ZnO/MgO ETL and the single ZnO ETL. (MgO layer thickness ~ 10 nm).

Sample	Dark Current at -1V (mA cm^{-2})	**Shunt Resistance (Ω cm^2)**
ITO/ZnO/PTB7-Th:ITIC-2F/Au	- 1.1	5.3 x 10^3
ITO/ZnO/**MgO**(10 nm)/PTB7-Th:ITIC-2F/Au	-1.3 x 10^{-1}	2.6 x 10^4
ITO/ZnO/PTB7-Th:$PC_{70}BM$/Au	- 5.1	1.29 x 10^4
ITO/ZnO/**MgO**(10 nm)/PTB7-Th:$PC_{70}BM$/Au	- 2.8 x 10^{-3}	4.94 x 10^5

Table S4: Variation of the extracted dark current density and shunt resistance of OPVs based on a single ZnO ETL vs the bilayer ZnO/MgO ETL (with MgO layer thickness ~ 10 nm).

To extract the shunt resistance from the dark current-voltage data we follow the procedure described by Brus et al.[1]. For full details of this procedure we refer the reader to reference 1. In brief, we assume the modified ideal diode equation that includes a component for shunt resistance and series resistance (often used to model inorganic semiconductors) in the dark:

$$J = J_0\left(\exp\left(\frac{q(V - JR_s)}{nkT}\right) - 1\right) + \frac{V - JR_s}{R_{sh}}$$

where J_0 is the saturation current density, n is the ideality coefficient, R_s is the series resistance, R_{sh} is the shunt resistance. We determine the shunt resistance from the voltage dependence of the differential resistance (dV/dJ), where the value of the shunt resistance is equal to the differential resistance in the vicinity of zero bias. An example differential resistance vs voltage plot comparing samples of single ZnO ETL and the bilayer ZnO/MgO ETL is shown in Figure S7. We refrain from attempting to extract the series resistance from the plot since, as shown by Servaites et al.[2] there are deviations in modelling OPVs in terms of the ideal diode equation assumption at high voltages. However, we expect that the series resistance of the ZnO/MgO(5000rpm) ETL is lower than the single ZnO ETL due to the observed increase of the fill factor in devices employing the bilayer ETL compared to those with a single ZnO ETL.

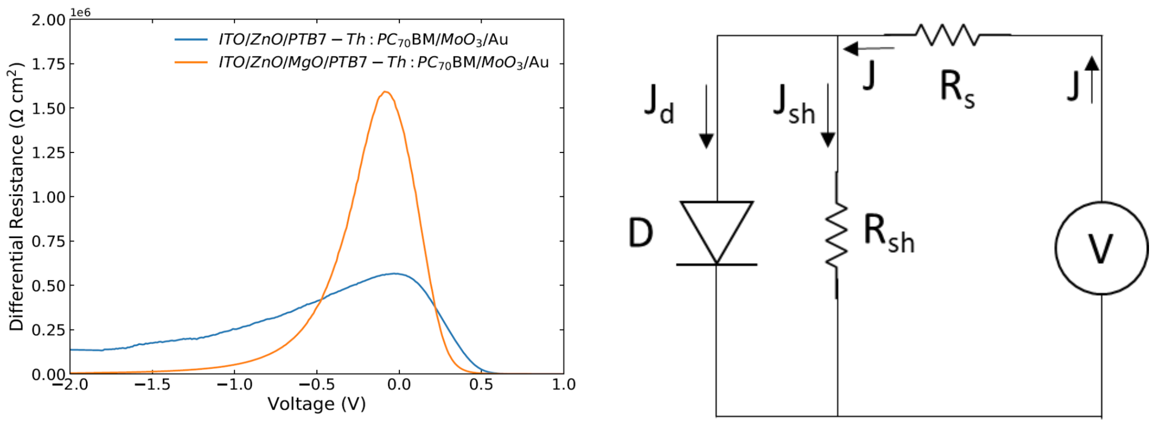

Figure S7: Example of a differential resistance vs voltage plot used to extract the shunt resistance and the equivalent circuit model employed.

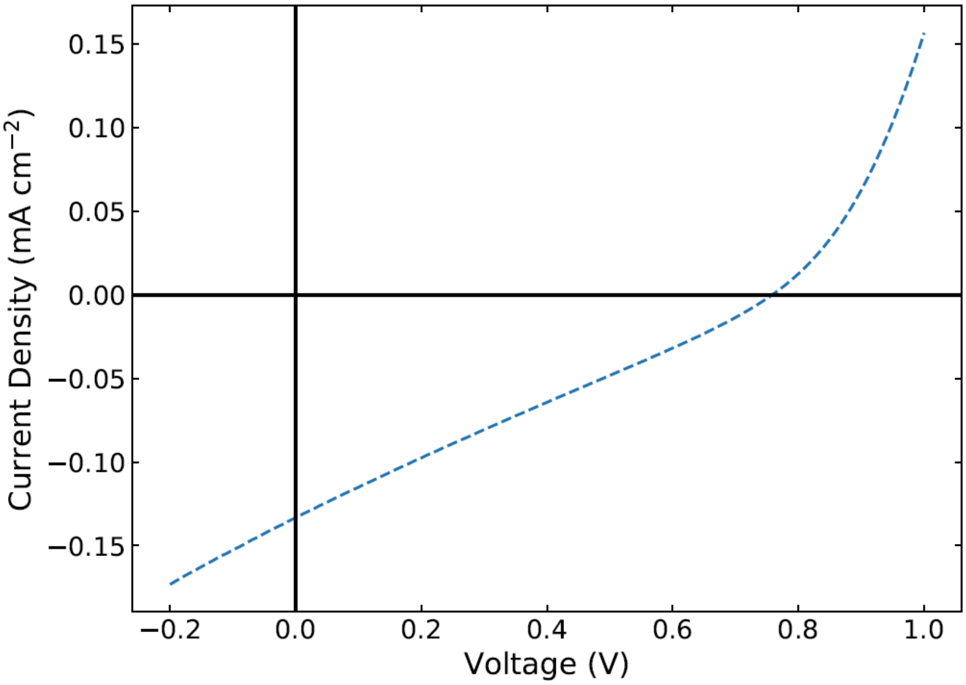

Figure S8: Representative current-voltage characteristics of ITO/ZnO/MgO/PTB7-Th:$PC_{70}BM$/MoO_3/Au samples, with the MgO layer deposited at 3000 rpm (thickness ≈150 nm). The much thicker layer of insulating MgO leads to severe loss in performance. The higher MgO thickness makes the extraction layer very resistive leading to a fill factor approaching 0.25 and to a small J_{sc}.

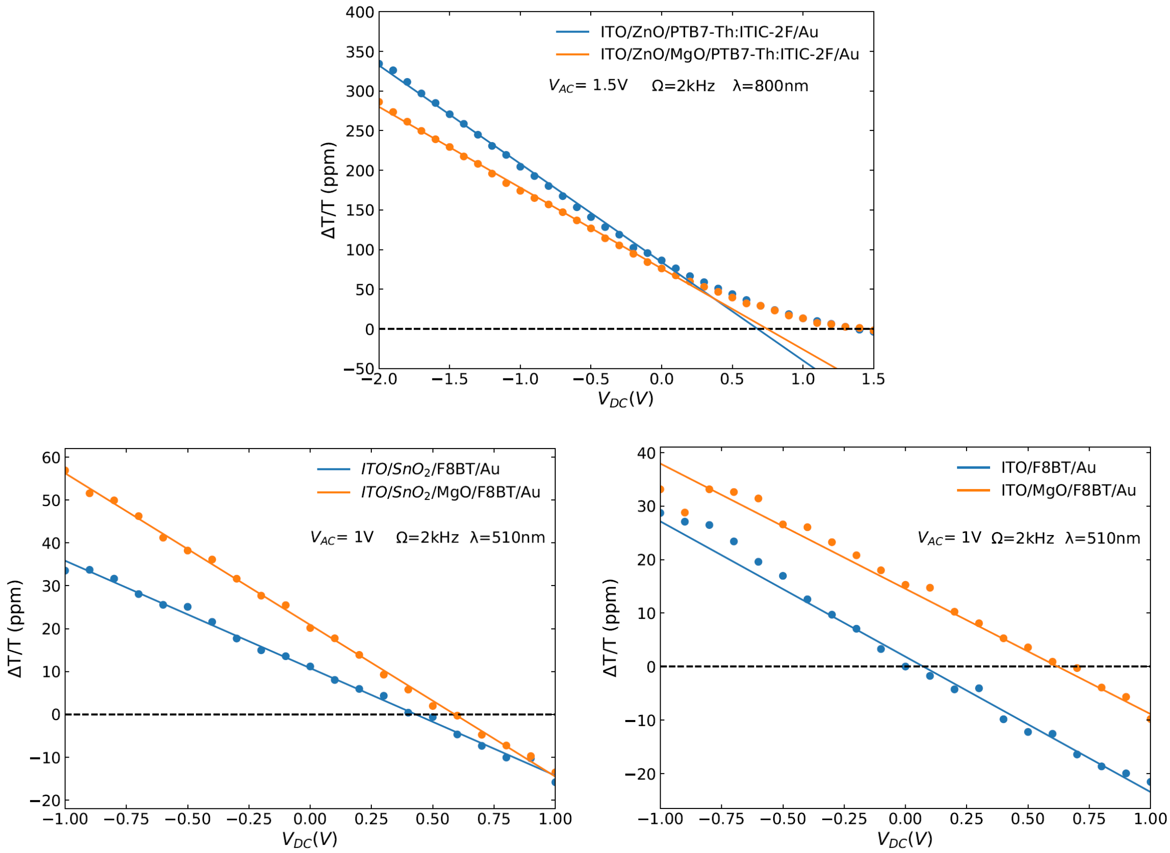

Figure S9: Electroabsorption signal vs DC voltage plots used to extract the built-in voltage in the single ETL and bilayer ETL devices. The experimental parameters used are displayed in the Figure (MgO layer thickness ~ 10 nm). F8BT rather than PTB7-Th:$PC_{70}BM$ was used as the active layer for the final two substrates as the purpose of these were to exhibit the effects of MgO addition rather than to be included in OPV devices (since these substrates were not optimised for this purpose).

<u>References:</u>

1. V. V. Brus, C. M. Proctor, N. A. Ran and T.-Q. Nguyen, Advanced Energy Materials, 2016, 6, 1502250.

2. J. D. Servaites, M. A. Ratner and T. J. Marks, Energy Environ.Sci., 2011, 4, 4410–4422.